

AD _____

Award Number: W81XWH-~~01~~ ~~FEH~~ ~~I~~

TITLE: T[^]~~ca~~ [~~3~~ ~~U~~ ~~c~~ [^] • ~~Q~~ ~~a~~ [~] & ~~a~~ [^] ~~A~~ [^] ~~E~~ ^{*} ~~a~~ ~~a~~ [^] ~~O~~ [^]] ~~!ca~~ } ~~Q~~ ~~a~~ [~] & [^] ~~A~~ [^] ~~E~~ ^c] @ ~~e~~ [^] ~~O~~ [^] || ~~O~~ [^] ~~a~~ ~~c~~ ~~Q~~ ~~A~~
Ú[• ~~ca~~ ~~O~~ ~~a~~ & [^]

PRINCIPAL INVESTIGATOR: Ö: ~~U~~ ~~a~~ ~~c~~ ~~a~~ ~~O~~ [~~a~~

CONTRACTING ORGANIZATION: University of ~~O~~ ~~a~~ ~~i~~ } ~~a~~ ~~O~~ ~~a~~ ~~a~~
~~O~~ ~~a~~ ~~a~~ ~~O~~ ~~a~~ ~~i~~ ~~i~~ ~~F~~ ~~i~~ ~~A~~

REPORT DATE: ~~E~~ ^{*} [~] • ~~O~~ ~~E~~ ~~F~~ ~~F~~

TYPE OF REPORT: Annual

PREPARED FOR: U.S. Army Medical Research and Materiel Command
Fort Detrick, Maryland 21702-5012

DISTRIBUTION STATEMENT: Approved for public release; distribution unlimited

The views, opinions and/or findings contained in this report are those of the author(s) and should not be construed as an official Department of the Army position, policy or decision unless so designated by other documentation.

REPORT DOCUMENTATION PAGE				Form Approved OMB No. 0704-0188	
Public reporting burden for this collection of information is estimated to average 1 hour per response, including the time for reviewing instructions, searching existing data sources, gathering and maintaining the data needed, and completing and reviewing this collection of information. Send comments regarding this burden estimate or any other aspect of this collection of information, including suggestions for reducing this burden to Department of Defense, Washington Headquarters Services, Directorate for Information Operations and Reports (0704-0188), 1215 Jefferson Davis Highway, Suite 1204, Arlington, VA 22202-4302. Respondents should be aware that notwithstanding any other provision of law, no person shall be subject to any penalty for failing to comply with a collection of information if it does not display a currently valid OMB control number. PLEASE DO NOT RETURN YOUR FORM TO THE ABOVE ADDRESS.					
1. REPORT DATE (DD-MM-YYYY) 01-08-2011		2. REPORT TYPE Annual		3. DATES COVERED (From - To) 1 AUG 2010 - 31 JUL 2011	
4. TITLE AND SUBTITLE Metabolic Stress Induced by Arginine Deprivation Induces Autophagy Cell Death in Prostate Cancer				5a. CONTRACT NUMBER	
				5b. GRANT NUMBER W81XWH-08-1-0385	
				5c. PROGRAM ELEMENT NUMBER	
6. AUTHOR(S) Dr. Richard Bold E-Mail: richard.bold@ucdmc.ucdavis.edu				5d. PROJECT NUMBER	
				5e. TASK NUMBER	
				5f. WORK UNIT NUMBER	
7. PERFORMING ORGANIZATION NAME(S) AND ADDRESS(ES) University of California, Davis Davis, CA 95618				8. PERFORMING ORGANIZATION REPORT NUMBER	
9. SPONSORING / MONITORING AGENCY NAME(S) AND ADDRESS(ES) U.S. Army Medical Research and Materiel Command Fort Detrick, Maryland 21702-5012				10. SPONSOR/MONITOR'S ACRONYM(S)	
				11. SPONSOR/MONITOR'S REPORT NUMBER(S)	
12. DISTRIBUTION / AVAILABILITY STATEMENT Approved for Public Release; Distribution Unlimited					
13. SUPPLEMENTARY NOTES					
14. ABSTRACT The primary purpose of this research grant is to provide the necessary preclinical data demonstrating that prostate cancer cells are auxotrophic for arginine and therefore targeting arginine metabolism is a novel therapeutic approach. The primary methodology involves cell culture with the characterization of the arginine requirements for prostate cancer cell growth and then determination of the effect of arginine depletion on cell growth and cell death. Furthermore, we have investigated the mechanism of cell death and observed that arginine deprivation in those cells auxotrophic for this semi-essential amino acid induces autophagy as a precursor to programmed cell death. Major findings to date include the observation that the majority of prostate cancer cell lines lack arginine-succinate synthetase (ASS), the critical enzyme in arginine biosynthesis. Furthermore, arginine deprivation in those cell lines lacking ASS induces autophagy as a precursor to non-apoptotic cell death. Inhibition of autophagy appears to stimulate the induction of cell death.					
15. SUBJECT TERMS Prostate cancer, autophagy, arginine deiminase					
16. SECURITY CLASSIFICATION OF:			17. LIMITATION OF ABSTRACT UU	18. NUMBER OF PAGES 20	19a. NAME OF RESPONSIBLE PERSON USAMRMC
a. REPORT U	b. ABSTRACT U	c. THIS PAGE U			19b. TELEPHONE NUMBER (include area code)

Table of Contents

	<u>Page</u>
Introduction.....	4
Body.....	4-6
Key Research Accomplishments.....	6-7
Reportable Outcomes.....	7
Conclusion.....	7
End of Period Reporting Requirements.....	8
References.....	8
Appendix.....	

Introduction

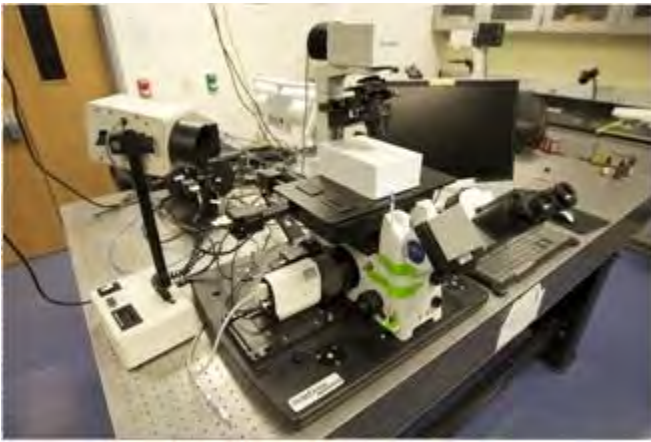
This is the third year of a three year grant entitled “Metabolic stress induced by arginine deprivation induces autophagy cell death in prostate cancer”. The **primary hypothesis** of the research investigation is PEG-ADI represents a potential therapy of prostate cancer to induce metabolic stress by arginine deprivation and subsequent induction of autophagic cell death as a precursor to apoptosis in those prostate cancers lacking biosynthetic enzymes to make arginine. The **specific aims** to investigate this hypothesis are:

- 1) We will demonstrate that in those prostate cancer cells lacking ASS for which arginine is an essential amino acid, metabolic stress induced by arginine deprivation achieved by ADI-PEG treatment induces autophagic cell death as a precursor to apoptosis via a DRAM-dependent pathway. From these studies, we will show: 1) ASS expression predicts cellular response to PEG-ADI, 2) PEG-ADI therapy induces arginine deprivation, 3) the consequence of the metabolic stress is the initiation of autophagosome assembly and progression to autophagic cell death, and 4) DRAM induction is required for PEG-ADI induced autophagy.
- 2) We will demonstrate that the induction of PEG-ADI induced autophagy in prostate cancer cells is a precursor to apoptosis; furthermore, these events sensitize cells to traditional chemotherapy-induced apoptosis. Autophagy mediators will be altered to determine effect on sensitivity to PEG-ADI induced cellular events. In addition, PEG-ADI will be combined with traditional chemotherapy to determine effect on apoptosis and in vivo tumor response.

Body

Significant progress has been accomplished during the third year of this 3-year award. The initial focus of the investigation was the characterization of the auxotrophic requirements for prostate cancer cell lines for the semi-essential amino acid arginine. These studies clearly demonstrated that only those prostate cancer cell lines lacking argininosuccinate synthetase (ASS) were sensitive to the cytotoxic effect of PEG-ADI (reference #3 below). Furthermore, PEG-ADI induced autophagy as well as a caspase-independent cell death (reference #4 below), though the relationship between these two cellular consequences of arginine are unclear. Therefore, the third year of the grant focused on the development of methodology to better investigate autophagy for more discrete quantitation using a deconvoluting microscope to assess single cell responses as well as the standardization of parameters for quantitation. In addition, we have characterized the effect of adding other autophagy-regulating agents on the cell death induced by PEG-ADI.

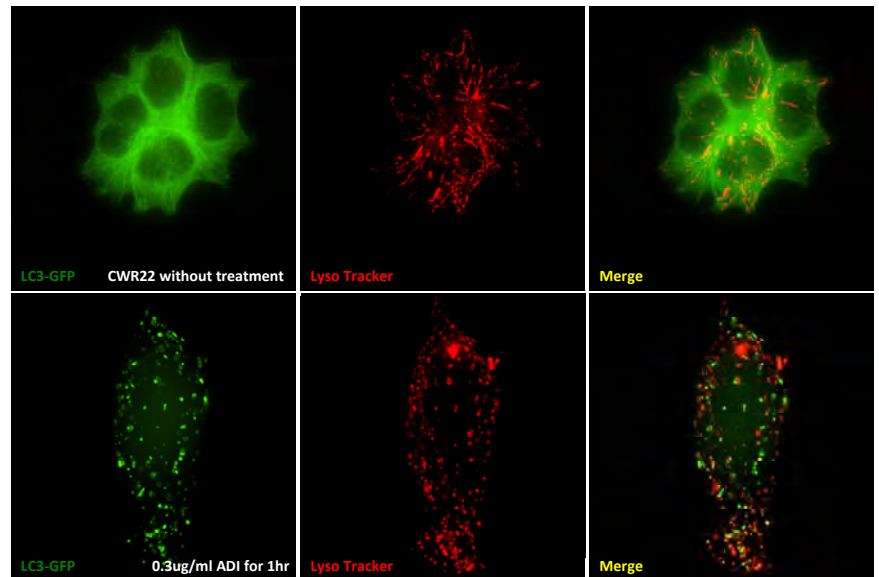
A significant amount of time was spent in the development of methodology to investigate autophagy. A current limitation in this field is the lack of methods that rely on crude evaluation of some of the very early biochemical events, but there are limitations in the depth or breadth of assays available. Therefore, we utilized the unique resources at UC Davis including the NSF-funded Center for Biophotonics, Science and Technology to develop a method to acquire real-time, single cell imaging of the cellular process of autophagy in response to PEG-ADI therapy of prostate cancer. CWR22Rv1 cells were stably transfected with a LC3-GFP construct to allow visualization of the LC3 protein, which undergoes processing in the early phases of autophagosome formation and can be detected by immunofluorescence (excitation 480 nM; emission 535 nM). Cells were subsequently loaded with LysoTracker Red to allow visualization by immunofluorescence (excitation 577 nM; emission 590 nM) of lysosome, which undergo fusion with the autophagosome during the terminal phases of autophagy.



Cells are then imaged on a personal deconvolution fluorescence microscope (Applied Precision, LLC, Issaquah, WA) for rapid live and fixed cell fluorescence microscopy. The system provides image-based auto-focusing and can image sample repeatedly over several days. Excitation/emission wavelengths are freely adjustable by swapping bandpass filters in a computer-controlled motorized filter wheel. This allows simultaneous imaging of both fluorescent markers over a time period of 120 minutes.

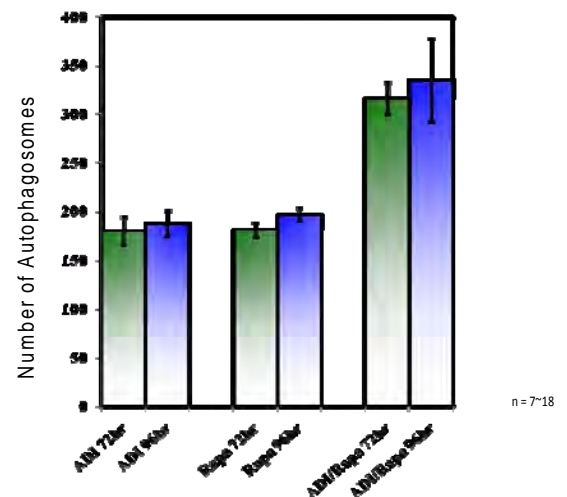
Deconvoluting Immunofluoresence of CWR22Rv1

Using this technique, cells were CWR22Rv1 cells were imaged following no treatment, or with PEG-ADI. As noted in the figure to the left in the absence of treatment, LC3 (green) is distributed diffusely in the cytoplasm, but when stimulated to undergo autophagy by PEG-ADI treatment, accumulate in autophagosomes (so call "punctae"). Furthermore, as observed in the far column, these autophagosomes co-localize with the lysosome (red staining) to yield yellow-stained vesicles following PEG-ADI treatment indicating the terminal phase of autophagy when the autophagosome fuses with the lysosome.

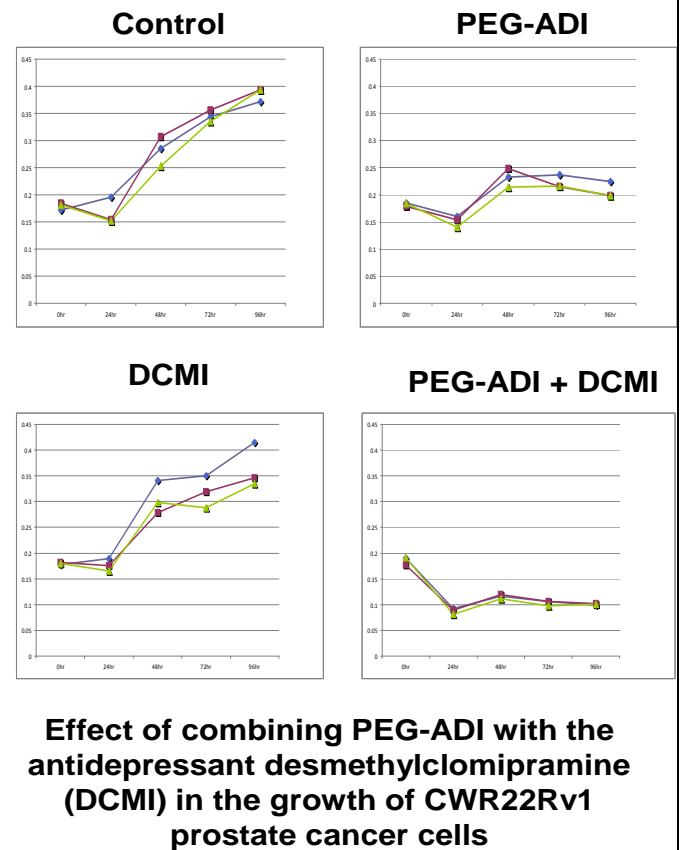


Using the associated software with this microscope, we were then able to more accurately quantify autophagy. By inputting variables to allow identification of the autophagosome (ie size, emission spectra, cellular location), we could determine the "amount" of autophagy in a cell. Rapamycin, an mTOR inhibitor well recognized to induce autophagy (data not shown and published by others extensively) was combined with PEG-ADI. In this circumstance, the cellular effect was increased cell death. Using this methodology, we noted that the cellular underwent "more" autophagy as demonstrated by an increase in the number of autophagosomes (determined by counting 7-18 individual cells at the time points shown. In addition, as we can image live cells, we were able to note that the initiation of autophagy occurs as early as 60 minutes following PEG-ADI treatment (data not shown).

ADI and Rapamycin Combo Treatment Produces Excessive Number of Autophagosomes in CWR22Rv1 Cells

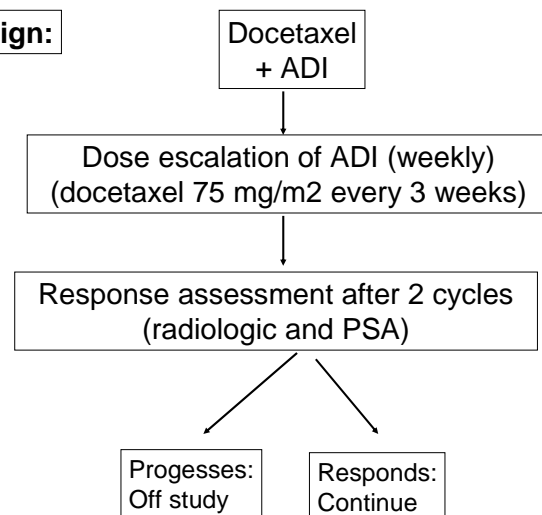


We have since begun exploring combinations of PEG-ADI with other agents that may regulate autophagy. One interesting combination uses the anti-depressant desmethylclomipramine (DCMI). As a selective serotonin reuptake inhibitor, the drug has recently been shown to inhibit autophagy. Thus, this agent represents another FDA-approved autophagy regulator but in contrast to rapamycin (an inducer of autophagy used in the above experiments), DCMI inhibits autophagy along the lines of chloroquine used in previous experiments. Unlike chloroquine, however, we noted that DCMI had little effect on the growth of CWR22Rv1 prostate cancer cells (left lower panel, right), but increased the cytotoxicity of PEG-ADI (right lower panel, right) as well as accelerating the time course of cell death. Therefore, a broad approach to autophagy induction may not be optimal for drug combinations with PEG-ADI. Additional detailed evaluation of autophagy regulators and predictors of response based on mechanism is planned for further rationale drug combination development.



Lastly, given our very convincing data combining PEG-ADI with docetaxel in a murine xenograft model of prostate cancer, we submitted an NIH grant (R21 mechanism to fund a human subjects protocol to conduct a Phase I study of this combination in hormone-refractory prostate cancer. Unfortunately this grant was not funded, so we pursued a contract with the biotechnology company that manufactures PEG-ADI, Polaris Pharmaceuticals. A contract has been signed between Polaris Pharmaceuticals and UC Davis to conduct a Phase I/II clinical trial of PEG-ADI + docetaxel in hormone-refractory prostate cancer. The protocol has received IRB approval and is anticipated to open in the very near future.

Design:



Key Research Accomplishments

1. Characterization of signaling pathways mediating autophagy and cell death following PEG-ADI in prostate cancer.
2. Development of real-time single cell imaging for assessment of autophagy.
3. Investigation of the interaction of autophagy and cell death mediated by PEG-ADI
4. Development of a new methodology for real time, single cell assessment of autophagy with

detailed determination of kinetics.

5. Initiation of a Phase I/II human clinical trial of PEG-ADI + docetaxel in metastatic, hormone-refractory prostate cancer.

Reportable Outcomes

Manuscripts:

1. Changou, A. G.P. McNerney, J.U. Jung, F.Y.S. Chuang, H-J. Kung **R.J. Bold**. Real time imaging using a deconvoluting microscope for single cell quantification of autophagy. Manuscript submitted, Autophagy.
2. Changou A., Kim, R.H., J.M. Coates, J.U. Jung, F.Y.S. Chuang, **R.J. Bold**, and H-J. Kung. Signaling pathways mediating autophagy induced by metabolic stress in human prostate cancer. Manuscript in preparation.
3. Changou A., F.Y.S. Chuang, **R.J. Bold**, and H-J. Kung. Impact of autophagy regulators on the cell death induced by arginine deprivation in prostate cancer auxotrophic for arginine. Manuscript in preparation.

Conclusion

In our third of a three year grant entitled “Metabolic stress induced by arginine deprivation induces autophagy cell death in prostate cancer”, we have made significant progress in the investigation of our central hypothesis. This has allowed us to move forward to a clinical trial of PEG-ADI in prostate cancer, which is a very noteworthy goal within 3 years of preclinical drug development. Furthermore, we have developed the methodology to more accurately quantitate autophagy as well as assess kinetics at the single cell level. Lastly, we have evaluated additional novel combinations of PEG-ADI with autophagy-regulating agents, which can be important information for additional drug development, as several of the agents (DCMI, chloroquine and rapamycin) are already in human use.

Therefore, the impact of the accomplishments of this research are several: 1) the preclinical evaluation of PEG-ADI sufficient to justify a human clinical trial, 2) the identification of autophagy as an alternative cellular mechanism that can be initiated by cancer therapies to initiate cell death, 3) the development of methodologies for the real-time, single cell assessment of autophagy.

As far as the financial conduct of the research, we are under budget without any significant deviations noted or anticipated. We have requested a one-year no cost extension (negotiated separately).

End of Reporting Supplemental Information

Research Personnel supported by this award

Richard Bold, MD (Principal Investigator)
Hsing-Jien Kung, PhD (Co-Investigator)
Julie Sutcliffe, PhD (Co-Investigator)
Subbulakshmi Virudachalam (Staff Research Associate)

Meeting Abstracts

1. Chuang FR, RH Kim, R Bold, HJ Kung. Measuring autophagic response using 4D image cytometry. 15th Annual UCD Cancer Research Symposium. Sept 2009.
2. RH Kim, F Chuang, G McNerney, J Coates, T Bowles, J Sutcliffe, R Jung, R Gandour-Edwards, R Bold, HJ Kung. Arginine deiminase: a novel therapy for prostate cancer and a tool to study quantitative autophagy. 15th Annual UCD Cancer Research Symposium. Sept 2009.
3. RH Kim, F Chuang, G McNerney, J Coates, T Bowles, J Sutcliffe, R Jung, R Gandour-Edwards, R Bold, HJ Kung. Arginine deiminase induces autophagic cell death in human prostate cancer. EMBO Conference: Autophagy-Cell biology, physiology and pathology. Oct 2009
4. Changou A, F Chuang, R Bold, HJ Kung. Use of a deconvoluting microscope to evaluate autophagy initiated by PEG-ADI in prostate cancer. UCD:Center for Biophotonics Science and Technology Annual Retreat. June 2010.
5. Changou A, F Chuang, HJ Kung, R Bold. Metabolic stress induces autophagy and caspase independent cell death in prostate cancer. DOD IMPACT Conference. 2011
6. Changou A, F Chuang, HJ Kung, R Bold. Image-based analysis of cell death by metabolic stress-induced autophagy. SPIE Photonics West BioS Meeting. Jan 2012

References

4. Kim, R.H., J.M. Coates, T.L. Bowles, G.P. McNerney, J. Sutcliffe, J.U. Jung, R. Gandour-Edwards, F.Y.S. Chuang, **R.J. Bold**, and H-J. Kung. Arginine deiminase as a novel therapy for prostate cancer induces autophagy and caspase-independent apoptosis. Cancer Research, 69(2):700-708, 2009. (Attached in Appendix)
5. Kim, R.H., **R.J. Bold**, and H-J. Kung. ADI, autophagy and apoptosis: Metabolic stress as a therapeutic option for prostate cancer. Autophagy. 5(4):567-8, 2009. (Attached in Appendix)
6. Changou, A. G.P. McNerney, J.U. Jung, F.Y.S. Chuang, H-J. Kung **R.J. Bold**. Real time immunofluorescence for imaging and quantification of autophagy. Manuscript in preparation.

Appendix

Arginine Deiminase as a Novel Therapy for Prostate Cancer Induces Autophagy and Caspase-Independent Apoptosis

Randie H. Kim,¹ Jodi M. Coates,² Tawnya L. Bowles,² Gregory P. McNerney,³ Julie Sutcliffe,⁴ Jae U. Jung,⁶ Regina Gandour-Edwards,⁵ Frank Y.S. Chuang,³ Richard J. Bold,² and Hsing-Jien Kung¹

Departments of ¹Biological Chemistry, ²Surgery (Division of Surgical Oncology), ³Biophysics (Center for Biophotonics and Science Technology), ⁴Biomedical Engineering, and ⁵Pathology, University of California at Davis, Sacramento, California; and ⁶Department of Molecular Microbiology and Immunology, University of Southern California Keck Medical School, Los Angeles, California

Abstract

Arginine deprivation as an anticancer therapy has historically been met with limited success. The development of pegylated arginine deiminase (ADI-PEG20) has renewed interest in arginine deprivation for the treatment of some cancers. The efficacy of ADI-PEG20 is directly correlated with argininosuccinate synthetase (ASS) deficiency. CWR22Rv1 prostate cancer cells do not express ASS, the rate-limiting enzyme in arginine synthesis, and are susceptible to ADI-PEG20 *in vitro*. Interestingly, apoptosis by 0.3 µg/mL ADI-PEG20 occurs 96 hours posttreatment and is caspase independent. The effect of ADI-PEG20 *in vivo* reveals reduced tumor activity by micropositron emission tomography as well as reduced tumor growth as a monotherapy and in combination with docetaxel against CWR22Rv1 mouse xenografts. In addition, we show autophagy is induced by single amino acid depletion by ADI-PEG20. Here, autophagy is an early event that is detected within 1 to 4 hours of 0.3 µg/mL ADI-PEG20 treatment and is an initial protective response to ADI-PEG20 in CWR22Rv1 cells. Significantly, the inhibition of autophagy by chloroquine and Beclin1 siRNA knockdown enhances and accelerates ADI-PEG20-induced cell death. PC3 cells, which express reduced ASS, also undergo autophagy and are responsive to autophagy inhibition and ADI-PEG20 treatment. In contrast, LNCaP cells highly express ASS and are therefore resistant to both ADI-PEG20 and autophagic inhibition. These data point to an interrelationship among ASS deficiency, autophagy, and cell death by ADI-PEG20. Finally, a tissue microarray of 88 prostate tumor samples lacked expression of ASS, indicating ADI-PEG20 is a potential novel therapy for the treatment of prostate cancer. [Cancer Res 2009;69(2):700–8]

Introduction

The initial observations that various tumor cells are susceptible to arginine deprivation were made over 40 years ago, although appropriate therapeutic methods have hindered further development of this approach until recently. Arginine deiminase (ADI), an enzyme isolated from *Mycoplasma* (1, 2), degrades arginine into its citrulline precursor. In its native form, it is strongly antigenic with

a half-life of 5 hours (3). Conjugation to 20,000 mw polyethylene glycol (ADI-PEG20) decreases antigenicity as well as dramatically increases serum half-life, allowing weekly administration that reduces plasma arginine to undetectable levels (4, 5). Various tumor types (hepatocellular carcinomas, melanomas, mesotheliomas, renal cell carcinomas, pancreatic carcinomas) have been shown to lack expression of argininosuccinate synthetase (ASS; refs. 4, 6–8), a ubiquitous enzyme involved in the two-step synthesis of arginine from citrulline (9). Unable to synthesize their own arginine, ASS-deficient cells depend on relatively inefficient amino acid transporters (10). In the setting of ASS deficiency, ADI-PEG20 depletes intracellular arginine by reducing extracellular levels available for transmembrane uptake while unaffected cells with preserved ASS expression capable of endogenous arginine biosynthesis (11). Previous *in vitro* studies show the growth of prostate cancer PC3 cells is inhibited when arginine is eliminated from cell culture medium (12), indicating ADI-PEG20 may be an effective therapy for prostate cancers.

The antitumor effects of ADI-PEG20 elicit a G₁ cell cycle arrest with eventual apoptosis in a number of tumor cell lines (13). In addition, ADI-PEG20 is antiangiogenic, inhibiting migration and tube formation in HUVE cells (14) and neovascularization of neuroblastomas *in vivo* (15). However, other cellular effects of arginine starvation by ADI-PEG20 are still unknown.

Nutrient depletion triggers a process called macroautophagy (hereafter called autophagy), an evolutionary conserved eukaryotic process in which organelles and bulk proteins are turned over by lysosomal activity. Autophagy serves to provide ATP and other macromolecules as energy sources during metabolic stress (16, 17). The most distinctive feature of autophagy is the formation of the autophagosome, a double-membrane vesicle that fuses with lysosomes for hydrolytic cleavage of engulfed proteins and organelles. In mammalian cells, microtubule-associated protein 1 light chain 3 (LC3) is processed by lipid conjugation to phosphatidylethanolamine for insertion into the autophagosome membrane (18). Translocation and processing of an eGFP-LC3 fusion protein are often used as markers for autophagic activity.

Autophagy has recently gained much attention for its paradoxical roles in cell survival and cell death, particularly in the pathogenesis as well as the treatment of cancer (19, 20). Regulation of autophagy is highly complex with inputs from the cellular environment through the phosphatidylinositol-3-OH kinase (PI3K)/Akt/mammalian target of rapamycin (mTOR) pathway (21), members of the Bcl2 family (22), p53 (23), and death-associated protein kinases (24). Not surprisingly, there is an intricate relationship between autophagy and apoptosis. Whether autophagy enables cells to survive or enhances their death is context-driven, depending on the type of stimuli, nutrient availability, organism

Requests for reprints: Hsing-Jien Kung, UC Davis Cancer Center, University of California - Davis Medical Center, Research III, Room 2400B, 4645 2nd Avenue, Sacramento, CA 95817. Phone: 916-734-1538; Fax: 916-734-2589; E-mail: hkung@ucdavis.edu and Richard J. Bold, University of California - Davis Medical Center, 4501 X Street, Sacramento, CA 95817. Phone: 916-734-5907; Fax: 916-703-5267; E-mail: richard.bold@ucdmc.ucdavis.edu.

©2009 American Association for Cancer Research.
doi:10.1158/0008-5472.CAN-08-3157

development, and apoptotic status. We hypothesize prostate cancer cells that are ASS deficient are sensitive to arginine deprivation by ADI-PEG20 and consequently, undergo autophagy as an initial survival response.

In this study, we show susceptibility of several prostate cancer cell lines to ADI-PEG20 correlates with the absence of ASS expression. Due to the lack of ASS, ADI-PEG20 induces a late caspase-independent cell death in CWR22Rv1 *in vitro*. Metabolic activity by micro positron emission tomography (microPET) imaging of CWR22Rv1 xenografts in nude mice was reduced by ADI-PEG20. Tumor growth was significantly inhibited by ADI-PEG20 alone as well as in combination with docetaxel. ADI-PEG20 also induces autophagy within hours of treatment. However, inhibition of autophagy prematurely leads to cell death by ADI-PEG20. With the success of ADI-PEG20 therapy for hepatocellular carcinomas and melanomas and our findings that prostate cancer specimens lack ASS expression, ADI-PEG20 can potentially be extended to clinical trials for prostate cancer. Moreover, combination with standard chemotherapies or autophagy-targeting drugs represents multipronged approaches to cancer therapy.

Materials and methods

Reagents. Recombinant ADI formulated with multiple linear 20,000 mw polyethylene glycol molecules (ADI-PEG20) was generously provided by DesignRx Pharmaceuticals, Inc. Specific enzyme activity was 7.4 IU/mg. Internal calibration of enzyme IC₅₀ was determined with each batch.

Cells and cell culture. All cell lines were cultured in RPMI 1640 [10% fetal bovine serum (FBS), 1% penicillin, streptomycin, glutamine]. LNCaP cells were cultured in serum-free, phenol-free medium before 10 nmol/L 5 α -Dihydrotestosterone (DHT; Sigma) treatment for 4, 24, and 48 h. PC3 cells were transiently transfected and CWR22Rv1 cells were stably transfected with eGFP-LC3 plasmid (JUI) using Effectene (Qiagen).

Reverse transcription-PCR and quantitative reverse transcription-PCR. Total RNA was isolated from cultured cells by TRIzol (Invitrogen) homogenization and reverse transcribed using Moloney murine leukemia virus (Invitrogen). One hundred nanograms of cDNA were PCR amplified as described previously (25). Primers: ASS (F) 5'-GACGCTATGTCCAGCAAAG-3' and (R) 5'-TTGCTTTGCGTACTCCATCAG-3'; glyceraldehyde-3-phosphate dehydrogenase (GAPDH; F) 5'-ACCACAGTCCATGCCATCAC-3' and (R) 5'-TCCACCACCCTGTTGCTGTA-3'. Total RNA from primary prostate tissues was reverse transcribed using SuperScriptIII (Invitrogen). One hundred nanograms of cDNA were amplified by iQ5 iCycler thermal cycler (Bio-Rad) and monitored by SYBRGreen (Invitrogen) for real-time PCR. Threshold cycle values were normalized against actin and analyzed using QGene software. Primers were as follows: ASS (F) 5'-TGAAATTTGCTGAGCTGTG-3' and (R) 5'-ATGTACACCTGGCCCTTGAG-3'; Actin (F) 5'-TCCTTAATGTCACGACGATTT-3' and (R) 5'-GAGCGCGGCTACAGCTT-3'.

Immunoblotting. Cellular lysates were resolved on SDS-PAGE and electrophoretically transferred to polyvinylidene difluoride membranes. Membranes were incubated with primary antibody followed by species-specific horseradish peroxidase secondary antibody. Immunoreactive material was detected by chemiluminescence (Pierce Laboratories). Antibodies were as follows: actin (Santa Cruz Biotechnology), ASS (BD Biosciences), caspase-3 (Biosource), GAPDH (Chemicon), tubulin (Sigma), Beclin1, phos-

pho-AMP kinase (Thr172), phospho-mTor (Ser2481), phospho-S6 kinase (Thr389), phospho-S6 (Ser235/236), LC3, extracellular signal-regulated kinase (ERK)1/2, and phospho-ERK1/2 (Cell Signaling).

3-(4,5-Dimethylthiazol-2-yl)-2,5-diphenyltetrazolium bromide cytotoxicity assay. RWPE-1, LNCaP, PC3, and CWR22Rv1 cells were seeded in 96-well plates and treated with serial dilutions of ADI-PEG20. After 6 d, thiazolyl blue tetrazolium bromide (MTT; Sigma) was added for a final concentration of 0.5 mg/mL. PC3 cells were treated for 3 d in 2% FBS. Formazan crystals were solubilized by 10% SDS. The IC₅₀ is the drug concentration at which 50% of cell growth is inhibited.

Fluorescence-activated cell sorting analysis for sub-G₁ DNA fragmentation. CWR22Rv1 cells were treated with 0.3 μ g/mL ADI-PEG20, 100 nmol/L paclitaxel (Sigma), or pretreated with 50 μ mol/L z-VAD-fmk (MBL International). Cells were analyzed by flow cytometry as described previously (8).

Active caspase-3 ELISA. CWR22Rv1 cells were seeded in 6-well plates and treated with 100 nmol/L paclitaxel or 0.3 μ g/mL ADI-PEG20 for 24 h. Treatment groups were compared with cells pretreated with 50 μ mol/L z-VAD-fmk for 2 h before assaying for activated caspase-3 by ELISA (R&D Systems).

MicroPET imaging. Nude mice with CWR22Rv1 s.c. xenografts were injected via tail vein with 120 mCi of ¹⁸F-FDG and imaged by PET as described previously (26) before and after 5 IU ADI-PEG20 treatment of 4 or 24 h. Standard uptake values (SUV) were computed by dividing the activity concentration in each voxel by the injected dose and multiplying by animal weight. Absolute uptake values of posttreatment images were normalized to pretreatment images before analysis.

Xenograft efficacy studies. For tumorigenesis, 1×10^6 CWR22Rv1 cells were injected s.c. into the bilateral flanks of male athymic BALB/c mice (Harlan Sprague-Dawley, Inc). Mice received weekly 0.5 mL i.p. injections of sterile PBS ($n = 4$), 10 mg/kg docetaxel ($n = 4$), 5 IU (225 μ g/mL) ADI-PEG20 ($n = 4$), or both 10 mg/kg docetaxel and 5 IU ADI-PEG20 (1 mL total volume; $n = 4$). Tumor dimensions were measured twice weekly. Tumor volumes were calculated by $V = 0.5236 (L \times W^2)$, L = length, W = width.

Fluorescence microscopy for LC3. CWR22Rv1 and PC3 cells overexpressing eGFP-LC3 were seeded on poly-lysine-coated coverslips. Cells were treated with 0.3 μ g/mL ADI-PEG20 for 4 or 24 h or 2 μ mol/L rapamycin for 4 h. Cells were fixed, mounted using SlowFade with 4',6-diamidino-2-phenylindole (DAPI; Invitrogen), and examined under a $\times 60$ lens on an Olympus BX61 motorized reflected fluorescence microscope with an AMCA filter (excitation, 350 nm; emission, 460 nm) for DAPI and FITC filter (excitation, 480 nm; emission, 535 nm) for eGFP-LC3 using SlideBook4.1 software (Intelligent Imaging Innovations).

For live cell imaging, CWR22Rv1 cells overexpressing eGFP-LC3 were plated on 35 mm #1 glass bottom dishes (WillCo Wells), treated with 0.3 μ g/mL ADI-PEG20, and imaged with an IX-71 inverted microscope with a $\times 100$ 1.40 NA oil objective (Olympus) and ASI 400 air stream incubator (NEVTEK) set to 37°C. Images were acquired using a spinning disc system.

Inhibition of autophagy. CWR22Rv1 cells were treated with 25 μ mol/L chloroquine (Sigma), 0.1 μ g/mL ADI-PEG20, or both for 24, 48, 72, and 96 h. LNCaP cells were treated as above except with 0.3 μ g/mL ADI-PEG20. Cells were analyzed by fluorescence-activated cell sorting (FACS) analysis as described previously.

CWR22Rv1 cells were seeded in 6-well plates then transiently transfected with 100 pmol eGFP siRNA (Ambion) or Beclin1 siRNA ON-TARGETplus SMARTpool (Dharmacon) using DharmaFECT

reagent (Dharmacon). Cells were treated with 0.3 $\mu\text{g/mL}$ ADI-PEG20 for 24 or 48 h the following day and analyzed by FACS analysis as described previously.

PC3 cells were treated with 0.3 $\mu\text{g/mL}$ ADI-PEG20, 5 $\mu\text{g/mL}$ ADI-PEG20, 1 mmol/L 3-methyladenine (3-MA; Sigma), or both for 24, 48, and 72 h and analyzed by MTT as described previously.

ASS immunohistochemistry. Formalin-fixed, paraffin-embedded archival material from 88 prostate tumors and 59 normal prostate samples were obtained. Tumors represent a range of Gleason grades (3+3 = 6 to 4+5 = 9). H&E-stained sections were made from

each block to define representative tumor regions, and a tumor microarray (TMA) was constructed. TMA paraffin blocks were sectioned at 4 μm and transferred to glass slides. Immunohistochemistry was performed using α -ASS monoclonal mouse antibody (DesignRx Pharmacologies) at 2.2 $\mu\text{g/mL}$. Normal liver was used as a positive control. Omission of primary antibody was used as negative control. Sections were counterstained with Gill's hematoxylin and fixed. Slides were independently examined by a board certified anatomic pathologist (RGE) thrice and scored by percentage of cells stained.

Results

Sensitivity to ADI-PEG20 correlates with ASS expression.

ASS expression in three commonly cultured prostate carcinoma cell lines (LNCaP, PC3, CWR22Rv1) was evaluated for mRNA and protein levels. LNCaP is androgen dependent, whereas PC3 and CWR22Rv1 are androgen independent. The normal immortalized cell line RWPE-1 was used to evaluate ASS expression in noncancerous prostate cells. All cell lines expressed ASS mRNA determined by reverse transcription-PCR (RT-PCR) except CWR22Rv1 (Fig. 1A). Quantitative real-time PCR of ASS mRNA in the prostate cancer cell lines revealed that, relative to CWR22Rv1, LNCaP and PC3 expressed ASS transcript 6.7 and 1.4 times greater, respectively. Western blot analysis showed CWR22Rv1 did not express ASS protein; in contrast, PC3 expressed moderate levels, whereas LNCaP and RWPE-1 expressed high levels of ASS (Fig. 1B). Disparity between ASS mRNA and protein levels is potentially attributed to nonproductive, alternatively spliced transcripts or pseudogenes.⁷ The relationship between androgen status and ASS expression was further examined by treating LNCaP cells with 10 nmol/L DHT (Fig. 1C), revealing androgens do not regulate ASS expression.

To evaluate the effect of ADI-PEG20 on prostate carcinoma, the previously described cell lines were treated with ADI-PEG20 over a broad dose range and assayed for cytotoxicity with MTT. CWR22Rv1 was the most sensitive to ADI-PEG20 with an IC_{50} of 0.3 $\mu\text{g/mL}$. PC3 was moderately sensitive to ADI-PEG20, whereas LNCaP and RWPE-1 were not responsive to ADI-PEG20 (Fig. 1D). Taken together, these data confirm that ASS protein levels inversely correlate with sensitivity to ADI-PEG20. CWR22Rv1 was subsequently chosen as the model cell line for future experiments.

ADI-PEG20 induces caspase-independent apoptosis in CWR22Rv1 *in vitro*. To study whether the reduced viability of CWR22Rv1 upon ADI-PEG20 treatment is due to cell growth arrest, apoptosis, or both, we subjected treated and untreated cells to FACS analysis. The sub-G₁ DNA content was used as an indicator of apoptosis induced by ADI-PEG20. CWR22Rv1 cells were treated with 0.3 $\mu\text{g/mL}$ ADI-PEG20 for 4, 24, 48, 72, and 96 hours. Apoptosis was not induced until 4 days posttreatment, when ~30% of cells had undergone apoptosis (Fig. 2A). Although DNA fragmentation is considered the defining end point in apoptosis, caspase cleavage is an early marker for classic apoptosis. Interestingly, cleavage of caspase-3 into its activated 17 kDa fragment was undetected after ADI-PEG20 (Fig. 2B).

Caspase-independent cell death was further investigated with z-VAD-fmk, a pan-caspase inhibitor. Caspase inhibition was confirmed with caspase-3 ELISA (Fig. 2C). z-VAD-fmk led to a 50%

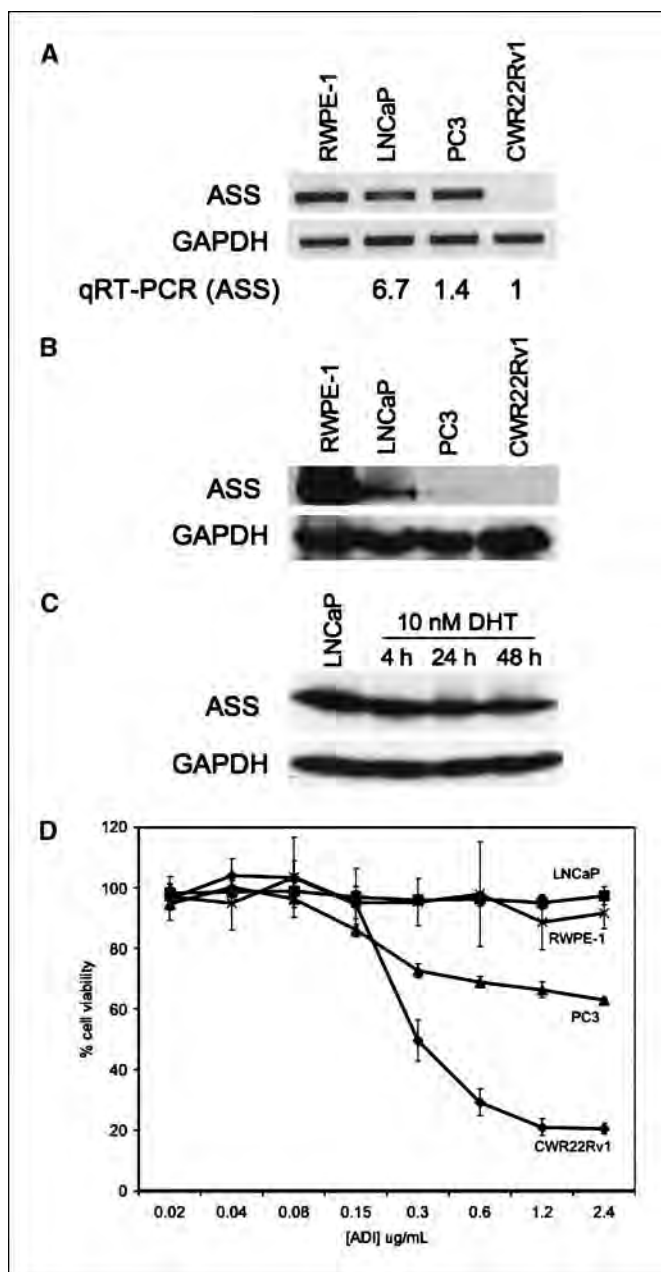


Figure 1. Prostate cancer cell lines profiled for ASS expression and ADI-PEG20 sensitivity. RWPE-1, LNCaP, PC3, and CWR22Rv1 were examined for ASS mRNA by RT-PCR (A) and ASS protein by immunoblotting (B). C, immunoblot for 10 nmol/L DHT time course of LNCaP against α -ASS. D, cell lines were treated by ADI-PEG20 at 0.02, 0.04, 0.08, 0.15, 0.3, 0.6, 1.2, and 2.4 $\mu\text{g/mL}$ for 3 (PC3) or 6 d before MTT assay. Points, mean; bars, SD.

⁷ Pei-Jer Chen, personal communication.

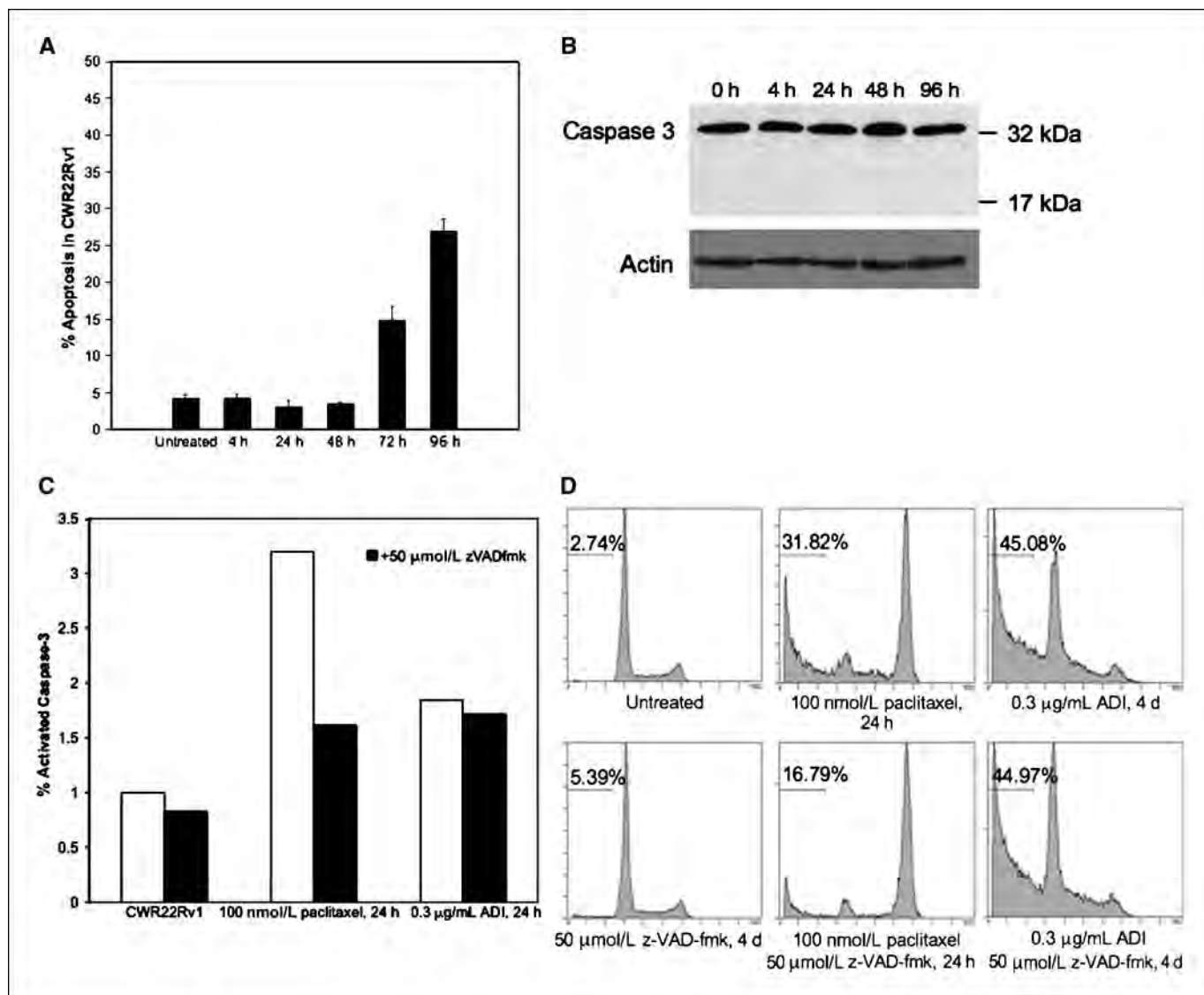


Figure 2. ADI-PEG20 induces caspase-independent apoptosis in CWR22Rv1. *A*, 0.3 μ g/mL ADI-PEG20 time course of CWR22Rv1 before FACS analysis for sub-G₁ DNA content. Columns, mean; bars, SE. *B*, immunoblot for 0.3 μ g/mL ADI-PEG20 time course of CWR22Rv1. α -Caspase-3 detects the 32 kDa proform and the activated 17 kDa cleavage product. *C*, CWR22Rv1 cells were treated with vehicle (untreated), 100 nmol/L paclitaxel, or 0.3 μ g/mL ADI-PEG20 for 24 h and compared with 2 h pretreatment with 50 μ mol/L z-VAD-fmk before caspase-3 ELISA. Values were normalized to vehicle. *D*, CWR22Rv1 cells were treated with 50 μ mol/L z-VAD-fmk, 0.3 μ g/mL ADI-PEG20, ADI-PEG20+z-VAD-fmk for 96 h, and 100 nmol/L paclitaxel, paclitaxel+z-VAD-fmk for 24 h before FACS analysis for sub-G₁ DNA content.

reduction of activated caspase-3 levels in cells treated with paclitaxel, a standard chemotherapy for advanced and metastatic prostate cancer. However, ADI-PEG20 did not significantly alter active caspase-3 levels. Although z-VAD-fmk attenuated apoptosis in cells treated with paclitaxel by ~50%, it did not affect the fraction of apoptotic cells after ADI-PEG20 (Fig. 2D). These data suggest that cell death mediated by ADI-PEG20 is independent of caspase-mediated pathways.

ADI-PEG20 decreases global tumor metabolic activity. The immediate effect of ADI-PEG20 *in vivo* was examined using PET. Global tumor metabolism of glucose consumption was monitored by ¹⁸F-fluorodeoxyglucose (¹⁸F-FDG) in CWR22Rv1 mouse xenografts. MicroPET scans were performed before and after ADI-PEG20 treatment of 4 or 24 hours. ¹⁸F-FDG uptake in CWR22Rv1 tumors (arrows) did not change after 4 hours of treatment. In

contrast, ¹⁸F-FDG uptake was decreased after 24 hours of ADI-PEG20. Tumor SUV decreased 30% after treatment (0.00086 versus 0.0006), indicating reduced metabolic activity (Fig. 3A).

ADI-PEG20 retards CWR22Rv1 tumor growth *in vivo* and synergizes with taxane. To determine the long term effects of ADI-PEG20 *in vivo*, nude athymic mice with s.c. CWR22Rv1 xenografts were injected i.p. with control PBS or 5 IU ADI-PEG20 weekly. Tumors from ADI-PEG20 mice were significantly smaller than tumors from control mice (157.6 mm³ versus 1,108.99 mm³) at 13 days after initiation of treatment when control mice were euthanized. The effects of ADI-PEG20 were compared with the current standard of care for hormone refractory prostate cancer patients, docetaxel alone (27), and docetaxel in combination. Docetaxel mice (10 mg/kg) had tumors that were smaller but not statistically significant from control mice. However, the

combination of ADI-PEG20 and docetaxel had a synergistic effect on tumor growth inhibition. Tumors from ADI-PEG20 mice reached an average of 910 mm³ at the end of the study, whereas tumors from ADI-PEG20/docetaxel-treated mice were ~75% smaller (Fig. 3B).

ADI-PEG20 induces autophagy in prostate cancer cells. Arginine degradation by ADI-PEG20 causes metabolic stress to auxotrophic cells. Nutrient starvation such as complete amino acid deprivation is a known inducer of autophagy (28). To determine whether single amino acid deprivation is sufficient to trigger autophagy, CWR22Rv1 cells stably expressing eGFP-LC3 were examined under fluorescence microscopy. Under normal conditions, LC3-I is uniformly distributed throughout the nucleus and cytoplasm. During autophagy, LC3-I is processed into LC-II and translocates into autophagosome membranes, appearing as bright punctae (29). LC3-II localization was seen in fixed CWR22Rv1 cells after 4 and 24 hours of 0.3 µg/mL ADI-PEG20 treatment. Rapamycin, an inhibitor of mTOR, was used as a positive control (Fig. 4A, top). Live cell imaging of CWR22Rv1 cells revealed rapid and intense autophagosome formation after only 90 minutes of ADI-PEG20 (Fig. 4A, bottom). Rapamycin or ADI-PEG20 significantly increased the number of cells undergoing autophagy to 15%

(Fig. 4A). The LC3-II fragment appeared as early as 30 minutes of ADI-PEG20 and persisted after 24 hours of arginine deprivation. Increase in total autophagic flux was confirmed with chloroquine (30), an autophagy inhibitor that disrupts lysosomal function (Fig. 4B) and prevents completion of autophagy, resulting in an accumulation of LC3-II. In addition, potential off-target effects of chloroquine did not lead to caspase-3 cleavage.

Molecular pathways accompanying the induction of autophagy were also investigated. A major nutrient-sensing pathway involves AMPK/TSC/mTOR/S6K. During nutrient starvation, ATP level decreases and AMP level increases, resulting in activation and phosphorylation of AMPK. ADI-PEG20 immediately increased phospho-AMPK levels (Fig. 4C). This should lead to inactivation and decreased phosphorylation of mTOR kinase through the inhibition of TSC complex by AMPK-induced phosphorylation. Decreased phosphorylation of mTOR was evident soon after ADI-PEG20 treatment (Fig. 4C). A downstream mTOR effector, S6K, was inactivated at a later stage (>24 hours) as shown by its own decreased phosphorylation and the decreased phosphorylation of its substrate S6. Transient increase of S6K activity was observed at early ADI-PEG20 time points. The exact mechanism of this phenomenon is unclear but is likely due to feedback of this kinase as reported by others (31). AMPK activation and mTOR down-modulation are compatible with their roles of major autophagy regulators. We also surveyed other kinase pathways relevant to autophagy. ERK1/2 phosphorylation was evident within 30 minutes of ADI-PEG20 treatment, which increased in a time-dependent manner (Fig. 4C). ERK1/2 activation has been shown previously to contribute to autophagy induced prosurvival function (32).

Autophagy delays and protects against ADI-PEG20-induced cell death. The paradoxical relationship between autophagy and apoptosis necessitates determination of the causal nature between these two fundamental biological processes after arginine deprivation. Temporally, autophagy precedes apoptosis; thus, inhibition of autophagy may modulate the onset of apoptosis.

Chemical inhibition of autophagy with chloroquine accelerated and enhanced ADI-PEG20-induced cell death in CWR22Rv1 (Fig. 5A). By 48 hours, 27% of ADI-PEG20 + chloroquine cells were apoptotic compared with 11% and 6% of cells undergoing apoptosis by chloroquine alone and ADI-PEG20 alone, respectively. Chloroquine further increased ADI-PEG20-induced cell death to 60% after 72 hours. By 96 hours, the effect of chloroquine was abrogated, possibly due to its metabolism. Similarly, siRNA knockdown of Beclin1, essential for autophagosome nucleation (21), also increased the rate of cell death after ADI-PEG20 treatment (Fig. 5B). Almost 60% of cells had undergone apoptosis if Beclin1 was knocked down before 48 hours of ADI-PEG20, whereas ADI-PEG20 alone only led to apoptosis in 30% of cells. In contrast, ADI-PEG20, chloroquine, and the combination of ADI-PEG20 and chloroquine had no effect on apoptosis at all time points in the ASS expressing LNCaP cells (Fig. 5C). To complete the characterization of the relationship of ASS expression and sensitivity to ADI-PEG20, we examined cellular response in PC3, a cell line with low ASS levels. Higher doses of ADI-PEG20 (5 µg/mL) were required to arrest cell growth completely compared with CWR22Rv1, although lower doses (0.3 µg/mL) induced autophagy (Fig. 5D). Inhibiting autophagy with 3-MA greatly reduced cell viability following treatment with low dose ADI-PEG20 (Fig. 5D). Therefore, ASS protein level correlates with cellular response to ADI-PEG20, including the early induction of autophagy before the late onset of apoptosis.

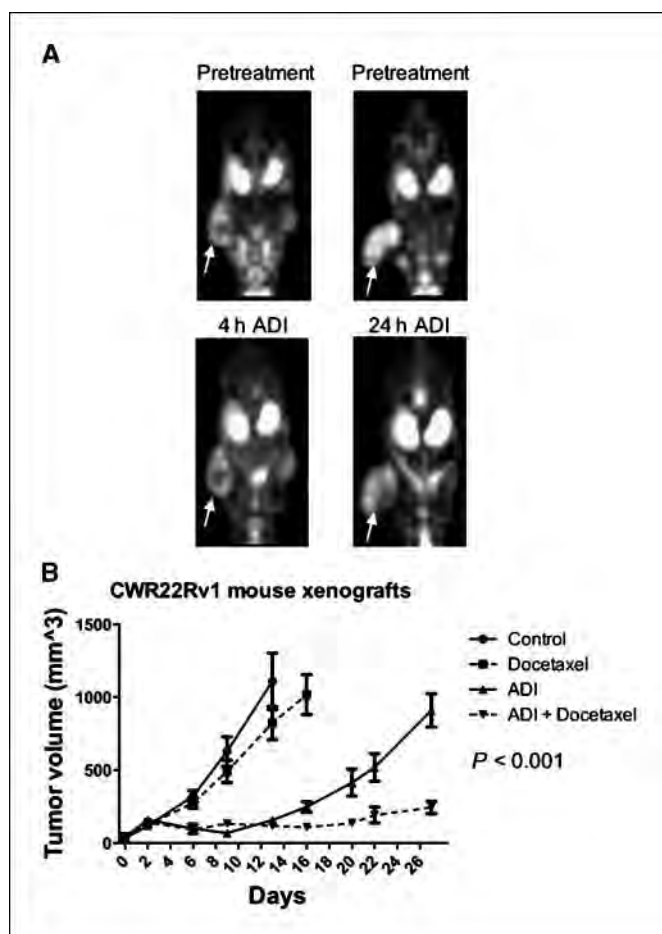
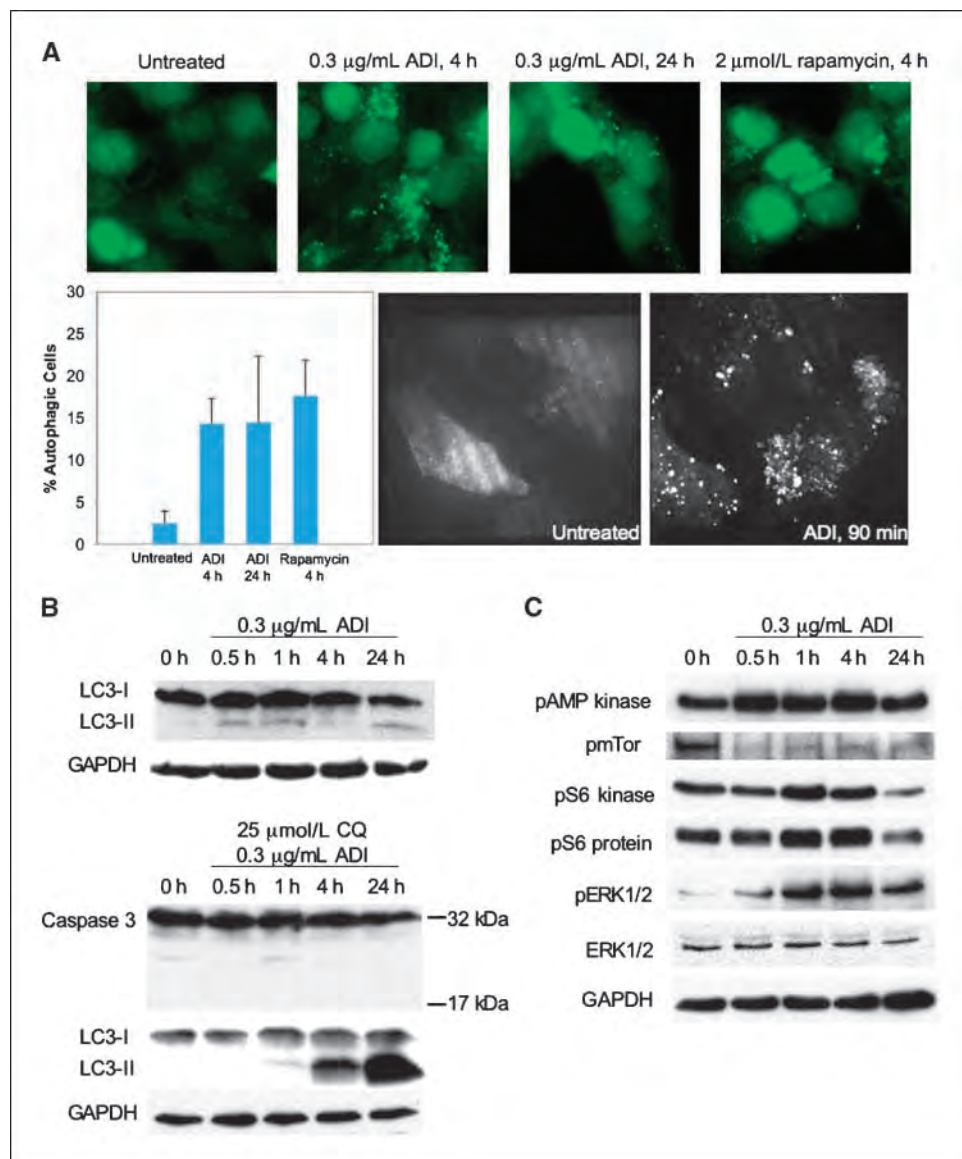


Figure 3. ADI-PEG20 is an effective agent *in vivo*. A, mice with CWR22Rv1 xenografts were imaged by PET using ¹⁸F-FDG before and after treatment with 5 IU ADI-PEG20 for 4 or 24 h. B, mice with CWR22Rv1 xenografts were treated with PBS vehicle, 10 mg/kg docetaxel, 5 IU ADI-PEG20, or 5 IU ADI-PEG20+10 mg/kg docetaxel weekly. Tumor volumes are reported as mean ± SE.

Figure 4. ADI-PEG20 induces autophagy in CWR22Rv1. **A**, CWR22Rv1 cells overexpressing eGFP-LC3 were treated with 0.3 $\mu\text{g/mL}$ ADI-PEG20 for 1.5, 4, and 24 h, or 2 $\mu\text{mol/L}$ rapamycin for 4 h. Punctae represent autophagosome formation. Autophagic cells were quantified from random image fields totaling 200 cells and reported as mean \pm SE. **B**, immunoblot for 0.3 $\mu\text{g/mL}$ ADI-PEG20 time course of CWR22Rv1. α -LC3 detects LC3-I and LC3-II. Autophagic flux was confirmed by coadministering 25 $\mu\text{mol/L}$ chloroquine with 0.3 $\mu\text{g/mL}$ ADI-PEG20. α -Caspase-3 detects the 32 kDa proform and the activated 17 kDa cleavage product. **C**, immunoblot for 0.3 $\mu\text{g/mL}$ ADI-PEG20 time course of CWR22Rv1 using α -phospho-AMP kinase, α -phospho-mTOR, α -phospho-S6 kinase, α -phospho-S6 protein, α -phospho-ERK1/2, and α -ERK1/2. Loading control for phospho-mTOR was verified using α -tubulin (data not shown).



ASS expression in prostate cancer tissue. The above results suggest arginine deprivation by ADI-PEG20 may offer a new treatment strategy for prostate cancers in which ASS expression is low. A key question that follows is whether the absence of ASS expression is generalizable among diverse human prostate cancer specimens. We therefore examined ASS expression by immunohistochemistry in our prostate tissue microarray. Of the 88 human prostate tumors, none showed any detectable ASS staining. Strong cytoplasmic ASS staining was observed, indicated by closed arrows, in the luminal cells of benign prostate glands (Fig. 6A) and normal prostate tissue (Fig. 6B, left). However, no ASS reactivity was detected in prostate cancer glands (Fig. 6A, open arrows) or tissue (Fig. 6B, right). Among 59 samples of normal prostate tissue, 27% expressed ASS to some degree. Of the 16 samples showing ASS expression, 2 were found to have ASS in >75% of the cells, whereas the remaining 14 showed expression in <25% of the cells. In addition, ASS mRNA expression was evaluated in six primary prostate tumor tissues and two primary benign prostatic hyperplasia tissues. ASS mRNA was almost absent in specimen

108 and reduced in all other samples (Fig. 6C). The differential expression of ASS is in contrast to hepatocytes, which heavily depend on ASS function for the urea cycle, and uniformly stained for cytoplasmic ASS protein (Fig. 6D).

Discussion

In this report, we showed ADI-PEG20 can effectively induce cell death in prostate cancer cells with low or absent ASS expression. It also sensitizes cells to treatment with docetaxel, an accepted chemotherapy in prostate cancer, or chloroquine, an inhibitor of autophagy. These results are likely to be generally applicable to other prostate cancer cells because virtually all prostate cancer specimens examined in this report as well as that by Clark and colleagues (12) expressed undetectable levels of ASS. By depletion of arginine, ADI-PEG20 causes metabolic stress on auxotrophic cells, complementing conventional therapies largely based on genotoxic stress. Although arginine deprivation therapy based on bovine arginase has seen limited applications clinically, ADI-PEG20

has 1,000-fold greater affinity for arginine (33) with fewer side effects. Our work described here thus offers a new treatment option for prostate cancer. In addition, we uncover novel cellular responses of arginine depletion, including autophagy and caspase-independent cell death.

The delayed onset of apoptosis suggests the possibility of compensation mechanisms after arginine depletion. Here, we present evidence for the first time that single amino acid starvation through arginine degradation by ADI-PEG20 is sufficient to trigger autophagy in prostate cancer cells. LC3 translocation and cleavage occur within hours of ADI-PEG20 treatment, indicating that autophagy is an early response. AMPK senses cellular AMP/ATP ratio, and in its phosphorylated form, signals the lack of nutrients in the environment to the mTOR complex via TSC2 (34). Inhibition of mTOR leads to suppression of S6K activity. Consistent with our findings, Feun and colleagues (35) have reported the effects of ADI-PEG20 on mTOR signaling, which include dephosphorylation of mTOR downstream effectors S6K and 4E-BP and increased phosphorylation of AMPK in ASS-negative melanoma cell lines. This chain of events has been shown to promote autophagy (36).

There are various signaling cascades that regulate mTOR/S6K including the PI3K (class I)/Akt pathway; inhibition of which has been shown to induce autophagy in malignant gliomas (32, 37). Although we did not specifically examine the activation of the PI3K (class I)/Akt pathway, ADI-PEG20 inhibited mTOR events associated with a rapid activation of AMPK, suggesting this mechanism in arginine deprivation-induced autophagy. Furthermore, we observed ADI-PEG20-induced ERK1/2 activation, which has been shown to regulate autophagy under a variety of stimuli (32, 38).

What is the biological function of ADI-PEG20 induced autophagy? Autophagy can be prosurvival or prodeath, depending on cellular context and duration of treatment. To study whether ADI-PEG20 induced autophagy contributes to or attenuates cell death, we chose to block ADI-PEG20 induced autophagy with the inhibitor chloroquine, which inhibits late stage autophagy by alkalinizing lysosomes and disrupting the autophagolysosome (39). Because chloroquine itself may have functions other than inactivating lysosomes (40), we also used siRNA targeting an essential component of autophagy, Beclin1, a component of the class III PI3 kinase complex that nucleates autophagosomes (29).

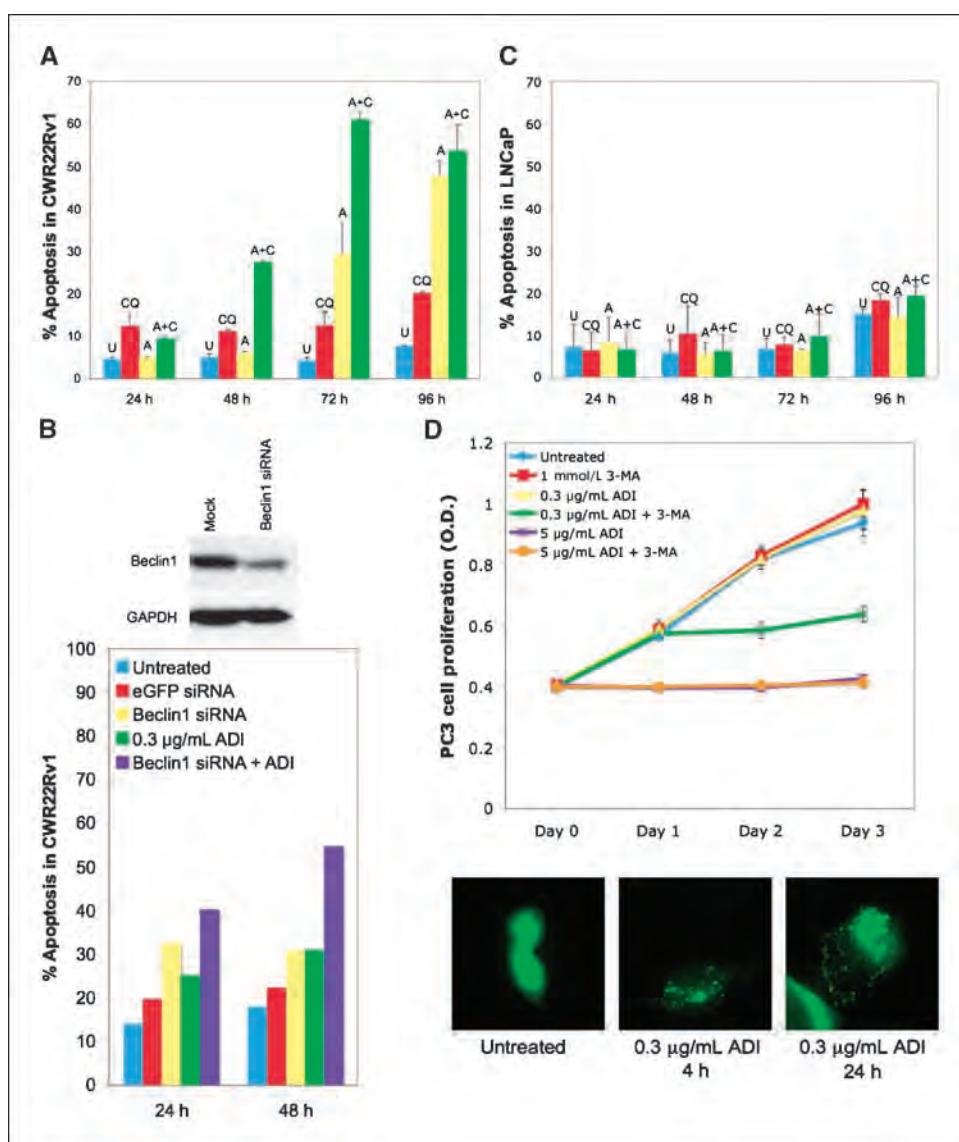
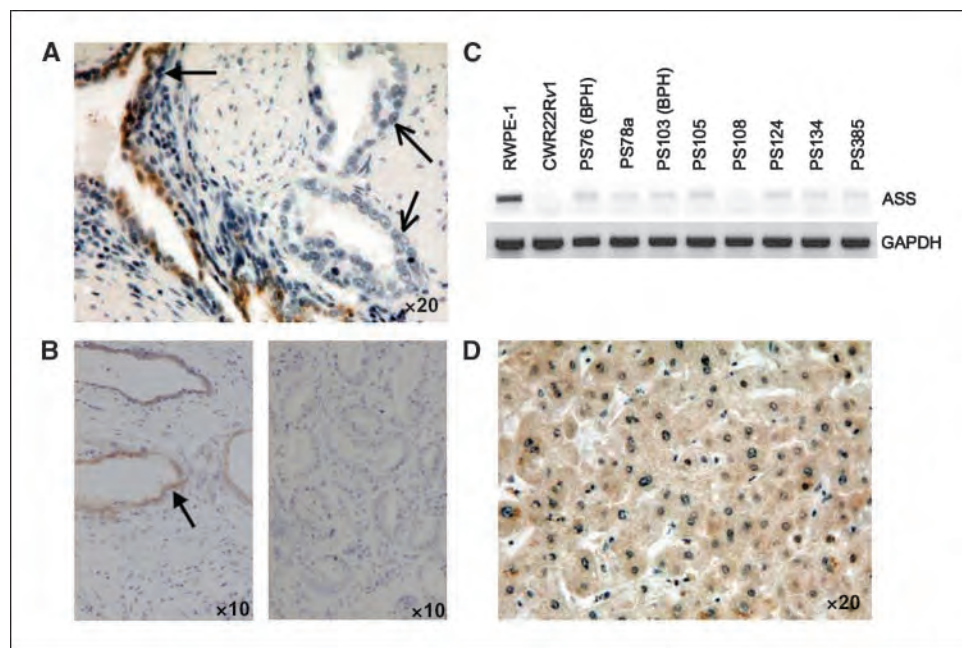


Figure 5. Inhibition of autophagy accelerates and enhances ADI-PEG20-induced cell death. *A*, time course of CWR22Rv1 cells treated with vehicle (untreated), 25 µmol/L CQ, 0.1 µg/mL ADI-PEG20, or ADI-PEG20+CQ before FACS analysis for sub-G₁ content. Columns, mean; bars, SE. *B*, immunoblot for CWR22Rv1 cells transfected with mock or 100 pmol Beclin1 siRNA to assess knockdown. CWR22Rv1 cells were treated with vehicle (untreated), 0.3 µg/mL ADI-PEG20, 100 pmol eGFP siRNA, 100 pmol Beclin1 siRNA, or Beclin1 siRNA+ADI-PEG20 for 24 and 48 h before FACS analysis for sub-G₁ content. *C*, LNCaP cells were treated and analyzed as described in *A* with 0.3 µg/mL ADI-PEG20. *D*, growth of PC3 cells were treated with vehicle (untreated), 0.3 µg/mL ADI-PEG20, 1 mmol/L 3-MA, 0.3 µg/mL ADI-PEG20+1 mmol/L 3-MA, 5 µg/mL ADI-PEG20, or 5 µg/mL ADI-PEG20+1 mmol/L 3-MA by MTT assay. Points, mean; bars, SD. PC3 cells overexpressing eGFP-LC3 were treated with 0.3 µg/mL ADI-PEG20 for 4 or 24 h. Punctae represent autophagosome formation. U, untreated; CQ, chloroquine; A, ADI-PEG20.

Figure 6. ASS expression in prostate tissue. *A*, prostate cancer tissue with ASS(+) benign glands (closed arrows) and ASS(−) cancerous glands (open arrows) by immunohistochemistry. *B*, left, normal prostate tissue. Closed arrows, luminal ASS staining. Right, prostate cancer tissue with no ASS reactivity. *C*, mRNA from primary prostate tissue was examined for ASS expression by RT-PCR. *D*, normal liver as a positive control for cytoplasmic ASS staining. *BPH*, benign prostatic hyperplasia.



Our data show inhibition of early stage autophagy by chloroquine or Beclin1 knockdown accelerates and enhances cell death after ADI-PEG20, strongly suggesting ADI-PEG20-induced autophagy triggers a protective response during early stages of treatment. At present, we cannot rule out that prolonged ADI-PEG20 treatment (>96 hours) may trigger autophagic cell death (programmed cell death type II), which is usually caspase-independent. In our study, we found chloroquine itself had little effect on the cell killing of CWR22Rv1, unless ADI-PEG20 is present and autophagy is induced. In addition, coadministration of chloroquine with ADI-PEG20 did not activate caspase-3. This again suggests that the major effect of chloroquine is to block autophagy, enhancing the underlying mechanism of caspase-independent apoptosis. Consistent with this result, PC3 cells with reduced ASS levels also underwent autophagy after ADI-PEG20 treatment. The inhibition of autophagy with 3-MA significantly reduced cell proliferation in the presence of ADI-PEG20. Both chloroquine and ADI-PEG20 have no effect on LNCaP cells, which express ASS. Interestingly, ASS-positive hepatocellular carcinomas resistant to ADI-PEG20 responded to arginine deprivation by pegylated recombinant arginase (41), providing a potential alternative to ADI-PEG20-resistant tumors and cell lines such as LNCaP.

In cancer, an autophagy paradox has emerged in which survival and death are context specific, particularly due to complex interactions between autophagic and apoptotic pathways. Accordingly, cancer therapies have been reported to have opposing effects on cell death. Photodynamic therapy promotes autophagic cell death in apoptosis-deficient cancer cells (42), whereas sulforaphane-induced autophagy in PC3 and LNCaP is protective (43). Furthermore, manipulation of autophagy can sensitize tumor cells to subsequent treatments. Induction of autophagy by an mTOR inhibitor increased prostate cancer cell susceptibility to irradiation (44). Conversely, chloroquine is a highly promising autophagy inhibitor for clinical use. Although it is extensively used to treat malaria (20), its uses against cancer are only recently emerging. In a *myc*-induced lymphoma model, autophagic

inhibition by chloroquine enhanced the ability of alkylating agents to suppress tumor growth (45). This underscores the importance of autophagy to fundamental cell processes and its ability to modulate the effect of chemotherapies across a wide variety of cancers.

The absence of ASS as a biomarker for ADI-PEG20 efficacy has previously been established in hepatoma and melanoma cell lines. Phase I/II clinical trials with ADI-PEG20 led to a 47% response rate in patients with unresectable hepatocellular carcinomas and a 25% response rate in metastatic melanoma patients (46, 47). In this study, we show ADI-PEG20 can be effective against prostate cancer. ASS expression can be determined by immunohistochemistry and potentially be used as a clinical indicator for ADI-PEG20 use. The absence of ASS protein in all examined prostate tumor samples makes ADI-PEG20 a promising therapeutic avenue to follow. The combination of ADI-PEG20, which induces caspase-independent apoptosis, and taxanes, which are caspase-dependent, is more effective than monotherapy. This concept of synergistic interaction between cancer therapies is an active area of research. In particular, combining therapies that target different mechanisms of cell death may increase efficacy beyond either agent alone. Furthermore, the increase of advanced imaging for tumor assessment and staging may allow clinical monitoring of tumor responsiveness to ADI-PEG20 by PET. Finally, arginine deprivation by ADI-PEG20 induces autophagy as a protective mechanism. Coadministration with an autophagic inhibitor such as chloroquine can potentially enhance cell death in prostate tumors. The intricate link between autophagy and apoptosis points to autophagy as an additional target for anticancer treatments. Thus, ADI-PEG20 is a novel prostate cancer therapy whose mechanism of action can be complemented by other chemotherapies to maximize cell death.

Disclosure of Potential Conflicts of Interest

R.J. Bold: commercial research grant, DesignRx Pharmaceuticals. The other authors disclosed no potential conflicts of interest.

Acknowledgments

Received 8/14/2008; revised 10/15/2008; accepted 10/31/2008.

Grant support: NIH DK52659 and CA114575 (H.J. Kung), 5TL1RR024145-02 (R.H. Kim); DOD W81XWH-08-1-0167 (R.H. Kim), and a research agreement by DesignRx Pharmaceuticals, Inc (R.J. Bold). H.J. Kung also acknowledges the support of the Auburn Community Cancer Endowment Fund.

References

- Miyazaki K, Takaku H, Umeda M, et al. Potent growth inhibition of human tumor cells in culture by arginine deiminase purified from a culture medium of a Mycoplasma-infected cell line. *Cancer Res* 1990;50:4522-7.
- Takaku H, Matsumoto M, Misawa S, Miyazaki K. Anti-tumor activity of arginine deiminase from Mycoplasma argini and its growth-inhibitory mechanism. *Jpn J Cancer Res* 1995;86:840-6.
- Takaku H, Takase M, Abe S, Hayashi H, Miyazaki K. *In vivo* anti-tumor activity of arginine deiminase purified from Mycoplasma arginini. *Int J Cancer* 1992;51:244-9.
- Ensor CM, Holsberg FW, Bomalaski JS, Clark MA. Pegylated arginine deiminase (ADI-SS PEG20,000 mw) inhibits human melanomas and hepatocellular carcinomas *in vitro* and *in vivo*. *Cancer Res* 2002;62:5443-50.
- Holsberg FW, Ensor CM, Steiner MR, Bomalaski JS, Clark MA. Poly(ethylene glycol) (PEG) conjugated arginine deiminase: effects of PEG formulations on its pharmacological properties. *J Control Release* 2002;80:259-71.
- Szlosarek PW, Klabatsa A, Pallaska A, et al. *In vivo* loss of expression of argininosuccinate synthetase in malignant pleural mesothelioma is a biomarker for susceptibility to arginine depletion. *Clin Cancer Res* 2006;12:7126-31.
- Yoon CY, Shim YJ, Kim EH, et al. Renal cell carcinoma does not express argininosuccinate synthetase and is highly sensitive to arginine deprivation via arginine deiminase. *Int J Cancer* 2007;120:897-905.
- Bowles TL, Kim R, Galante J, et al. Pancreatic cancer cell lines deficient in argininosuccinate synthetase are sensitive to arginine deprivation by arginine deiminase. *Int J Cancer* 2008;123:1950-5.
- Husson A, Brasse-Lagnel C, Fairand A, Renouf S, Lavoine A. Argininosuccinate synthetase from the urea cycle to the citrulline-NO cycle. *Eur J Biochem* 2003;270:1887-99.
- Lind DS. Arginine and cancer. *J Nutr* 2004;134:2837-41S; discussion 53S.
- Shen LJ, Beloussow K, Shen WC. Modulation of arginine metabolic pathways as the potential anti-tumor mechanism of recombinant arginine deiminase. *Cancer Lett* 2006;231:30-5.
- Dillon BJ, Prieto VG, Curley SA, et al. Incidence and distribution of argininosuccinate synthetase deficiency in human cancers: a method for identifying cancers sensitive to arginine deprivation. *Cancer* 2004;100:826-33.
- Gong H, Zolzer F, von Recklinghausen G, et al. Arginine deiminase inhibits cell proliferation by arresting cell cycle and inducing apoptosis. *Biochem Biophys Res Commun* 1999;261:10-4.
- Beloussow K, Wang L, Wu J, Ann D, Shen WC. Recombinant arginine deiminase as a potential anti-angiogenic agent. *Cancer Lett* 2002;183:155-62.
- Gong H, Pottgen C, Stuben G, Havers W, Stuschke M, Schweigerer L. Arginine deiminase and other antiangiogenic agents inhibit unfavorable neuroblastoma growth: potentiation by irradiation. *Int J Cancer* 2003;106:723-8.
- Levine B, Klionsky DJ. Development by self-digestion: molecular mechanisms and biological functions of autophagy. *Dev Cell* 2004;6:463-77.
- Mizushima N, Levine B, Cuervo AM, Klionsky DJ. Autophagy fights disease through cellular self-digestion. *Nature* 2008;451:1069-75.
- Kabeya Y, Mizushima N, Ueno T, et al. LC3, a mammalian homologue of yeast Apg8p, is localized in autophagosomal membranes after processing. *EMBO J* 2000;19:5720-8.
- Mathew R, Karantza-Wadsworth V, White E. Role of autophagy in cancer. *Nat Rev Cancer* 2007;7:961-7.
- Amaravadi RK, Thompson CB. The roles of therapy-induced autophagy and necrosis in cancer treatment. *Clin Cancer Res* 2007;13:7271-9.
- Pattingre S, Espert L, Biard-Piechaczky M, Codogno P. Regulation of macroautophagy by mTOR and Beclin 1 complexes. *Biochimie* 2008;90:313-23.
- Maiuri MC, Criollo A, Tasdemir E, et al. BH3-only proteins and BH3 mimetics induce autophagy by competitively disrupting the interaction between Beclin 1 and Bcl-2/Bcl-X(L). *Autophagy* 2007;3:374-6.
- Crichton D, Wilkinson S, O'Prey J, et al. DRAM, a p53-induced modulator of autophagy, is critical for apoptosis. *Cell* 2006;126:121-34.
- Gozuacik D, Kimchi A. DAPK protein family and cancer. *Autophagy* 2006;2:74-9.
- Desai SJ, Ma AH, Tepper CG, Chen HW, Kung HJ. Inappropriate activation of the androgen receptor by nonsteroids: involvement of the Src kinase pathway and its therapeutic implications. *Cancer Res* 2006;66:10449-59.
- Parsons CM, Sutcliffe JL, Bold RJ. Preoperative evaluation of pancreatic adenocarcinoma. *J Hepatobiliary Pancreat Surg* 2008;15:429-35.
- Van Poppel H. Recent docetaxel studies establish a new standard of care in hormone refractory prostate cancer. *Can J Urol* 2005;12 Suppl 1:81-5.
- Mortimore GE, Schworer CM. Induction of autophagy by amino-acid deprivation in perfused rat liver. *Nature* 1977;270:174-6.
- Liang C, Feng P, Ku B, et al. Autophagic and tumour suppressor activity of a novel Beclin1-binding protein UVRAG. *Nat Cell Biol* 2006;8:688-99.
- Mizushima N, Yoshimori T. How to interpret LC3 immunoblotting. *Autophagy* 2007;3:542-5.
- Codogno P, Meijer AJ. Autophagy and signaling: their role in cell survival and cell death. *Cell Death Differ* 2005;12 Suppl 2:1509-18.
- Shinojima N, Yokoyama T, Kondo Y, Kondo S. Roles of the Akt/mTOR/p70S6K and ERK1/2 signaling pathways in curcumin-induced autophagy. *Autophagy* 2007;3:635-7.
- Dillon BJ, Holsberg FW, Ensor CM, Bomalaski JS, Clark MA. Biochemical characterization of the arginine degrading enzymes arginase and arginine deiminase and their effect on nitric oxide production. *Med Sci Monit* 2002;8:BR248-53.
- Hardie DG. The AMP-activated protein kinase pathway-new players upstream and downstream. *J Cell Sci* 2004;117:5479-87.
- Feun L, You M, Wu CJ, et al. Arginine deprivation as a targeted therapy for cancer. *Curr Pharm Des* 2008;14:1049-57.
- Xu ZX, Liang J, Haridas V, et al. A plant triterpenoid, avicin D, induces autophagy by activation of AMP-activated protein kinase. *Cell Death Differ* 2007;14:1948-57.
- Aoki H, Takada Y, Kondo S, Sawaya R, Aggarwal BB, Kondo Y. Evidence that curcumin suppresses the growth of malignant gliomas *in vitro* and *in vivo* through induction of autophagy: role of Akt and extracellular signal-regulated kinase signaling pathways. *Mol Pharmacol* 2007;72:29-39.
- Pattingre S, Bauvy C, Codogno P. Amino acids interfere with the ERK1/2-dependent control of macroautophagy by controlling the activation of Raf-1 in human colon cancer HT-29 cells. *J Biol Chem* 2003;278:16667-74.
- Maiuri MC, Zalckvar E, Kimchi A, Kroemer G. Self-eating and self-killing: crosstalk between autophagy and apoptosis. *Nat Rev* 2007;8:741-52.
- Maclean KH, Dorsey FC, Cleveland JL, Kastan MB. Targeting lysosomal degradation induces p53-dependent cell death and prevents cancer in mouse models of lymphomagenesis. *J Clin Invest* 2008;118:79-88.
- Cheng PN, Lam TL, Lam WM, et al. Pegylated recombinant human arginase (rhArg-peg5,000mw) inhibits the *in vitro* and *in vivo* proliferation of human hepatocellular carcinoma through arginine depletion. *Cancer Res* 2007;67:309-17.
- Xue LY, Chiu SM, Azizuddin K, Joseph S, Oleinick NL. Protection by Bcl-2 against apoptotic but not autophagic cell death after photodynamic therapy. *Autophagy* 2008;4:125-7.
- Herman-Antosiewicz A, Johnson DE, Singh SV. Sulforaphane causes autophagy to inhibit release of cytochrome C and apoptosis in human prostate cancer cells. *Cancer Res* 2006;66:5828-35.
- Cao C, Subhawong T, Albert JM, et al. Inhibition of mammalian target of rapamycin or apoptotic pathway induces autophagy and radiosensitizes PTEN null prostate cancer cells. *Cancer Res* 2006;66:10040-7.
- Amaravadi RK, Yu D, Lum JJ, et al. Autophagy inhibition enhances therapy-induced apoptosis in a Myc-induced model of lymphoma. *J Clin Invest* 2007;117:326-36.
- Izzo F, Marra P, Beneduce G, et al. Pegylated arginine deiminase treatment of patients with unresectable hepatocellular carcinoma: results from phase I/II studies. *J Clin Oncol* 2004;22:1815-22.
- Ascierto PA, Scala S, Castello G, et al. Pegylated arginine deiminase treatment of patients with metastatic melanoma: results from phase I and II studies. *J Clin Oncol* 2005;23:7660-8.

Autophagic Punctum

ADI, autophagy and apoptosis

Metabolic stress as a therapeutic option for prostate cancer

Randie H. Kim,¹ Richard J. Bold² and Hsing-Jien Kung^{1,*}

¹Department of Biological Chemistry; ²Department of Surgery (Division of Surgical Oncology); University of California-Davis; Sacramento, CA USA

Key words: autophagy, arginine deiminase, arginine deprivation, caspase-independent apoptosis, prostate cancer

Prostate cancer, the leading incidence of cancer in American males, is a disease in which treatment of nonlocalized tumors remains largely unsuccessful. These cancers lose expression of an arginine synthesis enzyme, argininosuccinate synthetase (ASS), and are susceptible to arginine deprivation by arginine deiminase (ADI). We show CWR22Rv1 prostate cancer cells are susceptible to ADI in a caspase-independent manner in vitro and in a xenograft model in vivo. We demonstrate that single amino acid deprivation by ADI is able to trigger autophagy. Inhibition of autophagy by chloroquine and siRNA enhances and accelerates ADI-induced cell death, suggesting that autophagy is a protective response to ADI, at least in the early phases. In addition, the co-administration of docetaxel, a caspase-dependent chemotherapy, with ADI inhibits tumor growth in vivo. Thus, targeting multiple cell death pathways, either through autophagy modulation or non-canonical apoptosis, may find expanded use as adjuvant chemotherapies, providing additional avenues for cancer treatment.

Recently, there is renewed interest in agents that cause metabolic stress as an alternative or adjunctive therapy for cancer to overcome resistance to conventional genotoxic agents. Amino acid deprivation as an anticancer therapy has long been recognized. A well-known example is asparagine-deprivation by asparaginase for acute lymphoblastic leukemias. Similarly, arginase-based treatment for lymphosarcoma and hepatoma has been reported in experimental models. Arginase, however, has received little attention clinically, due to sub-optimal properties of the purified enzyme from bovine tissues. Arginine is a semi-essential amino acid that is manufactured by the enzyme ASS (argininosuccinate synthetase) (Fig. 1). For

reasons not well understood, in the development of certain cancers there is a selection against ASS expression, rendering the cancer cells auxotrophic for arginine. Consequently, arginine depletion by either arginase or arginine deiminase (ADI) will lead to selective tumor cell death.

ADI is an enzyme isolated from *Mycoplasma* that effectively metabolizes arginine into citrulline. At physiological pH, ADI is 300x more effective than arginase at depleting arginine. Antigenicity is decreased by conjugation to polyethylene glycol (PEG), which also increases enzyme half-life. Pegylated modification of recombinant ADI (DesignRx, California) has dramatically improved its prospects as a therapeutic agent. PEG-ADI is efficacious against hepatocellular carcinomas and melanomas in vitro and in vivo. In particular, phase I/II clinical trials in these patients yield significant response rates with mild side effects. The efficacy of ADI on hepatocellular carcinomas and melanomas is correlated with ASS deficiency. Strikingly, in our analysis of 88 prostate cancer specimens, none expressed ASS. Figure 2 illustrates the lack of ASS expression in tumor cells compared to the high expression found in the surrounding normal prostate epithelium.

We first tested the ADI effect on various prostate cancer cell lines and found ADI sensitivity was inversely proportional to ASS protein levels. CWR22Rv1, a castration-resistant prostate cancer cell line that does not express ASS, is highly sensitive to ADI-induced killing. We then extended these studies in vivo with CWR22Rv1 xenografts in nude mice. Weekly injections of ADI resulted in the complete suppression of tumor growth, indicating the effectiveness of ADI as a treatment option for prostate cancer.

The ADI-induced cell killing of CWR22Rv1 is atypical in at least two aspects: first, it is caspase-independent, and second, it follows a delayed kinetics with very little cell killing in the first 48 hours. Although nutritional starvation is known to induce autophagy, the effect of single amino acid removal such as arginine has not been as well documented. We therefore set forth to test whether ADI induces autophagy in CWR22Rv1. By GFP-LC3 (a marker for autophagosomes) under fluorescence microscopy and the generation of LC3-II by western, the induction of autophagy was detected as early as 30 minutes after ADI treatment. Time-lapse images of CWR22Rv1 cells overexpressing GFP-LC3 and RFP-LAMP-1 (a marker for lysosomes) using live cell fluorescence microscopy revealed the rapid appearance of large, bright puncta as well as dynamic colocalization with lysosomes over time (Fig. 3). Advanced quantitative parameters

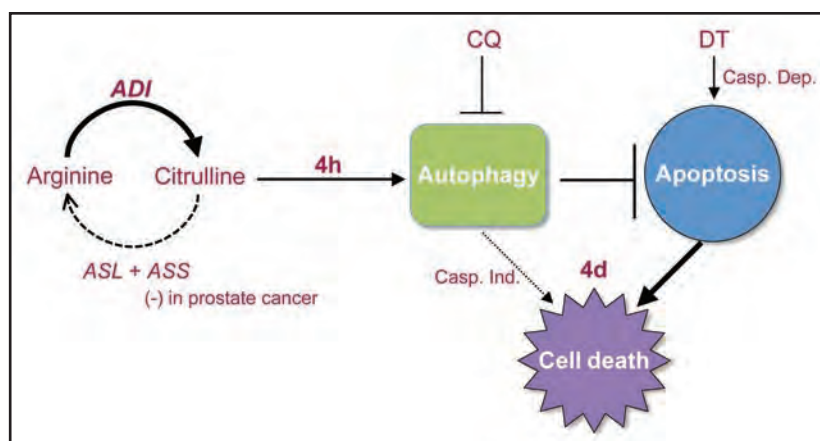
*Correspondence to: Hsing-Jien Kung; UC Davis Cancer Center; University of California—Davis Medical Center; Research III; Room 2400B; 4645 2nd Avenue; Sacramento, CA 95817 USA; Tel.: 916.734.1538; Fax: 916.734.2589; Email: hkung@ucdavis.edu

Submitted: 02/04/09; Revised: 02/19/09; Accepted: 02/20/09

Previously published online as an *Autophagy* E-publication:
<http://www.landesbioscience.com/journals/autophagy/article/8252>

Punctum to: Kim RH, Coates JM, Bowles TL, McNerney GP, Sutcliffe J, Jung JU, Gaudour-Edwards R, Chuang FYS, Bold RJ, Kung HJ. Arginine deiminase as a novel therapy for prostate cancer induces autophagy and caspase-independent apoptosis. *Cancer Res* 2009; 69:700-708; PMID: 19147587; DOI: 10.1158/0008-5472.CAN-08-3157.

Figure 1. Proposed model of ADI-induced cell death. Arginine is synthesized in a two-step process catalyzed by the rate-limiting enzyme argininosuccinate synthetase (ASS) and argininosuccinate lyase (ASL). Arginine deiminase (ADI) hydrolyzes arginine back into its citrulline precursor (solid arrow). In prostate tumors that lack ASS, citrulline cannot re-enter the arginine synthesis pathway (dashed arrow), resulting in the depletion of intracellular arginine and the accumulation of citrulline upon ADI treatment. ADI treatment leads to a rapid induction of autophagy (4 hours) as a protective response to delay apoptosis at 4 days. Prolonged autophagy, however, may also contribute to caspase-independent cell death (dotted arrow). Cell death can be enhanced using chloroquine (CQ), an autophagic inhibitor, or docetaxel (DT), a caspase-dependent apoptotic inducer.



extracted from 4D images of autophagosomes may reflect potentially different mechanistic pathways of autophagy. Detailed analysis of ADI-treated CWR22Rv1 cells revealed AMPK and ERK activation, and AKT, mTOR and S6K attenuation. Cells can, therefore, mount a strong autophagic response even to single amino acid depletion.

The relationship between autophagy and apoptosis after ADI treatment was investigated. siRNA knockdown of *beclin 1* enhanced ADI-induced apoptosis at both 24 and 48 hours, suggesting that autophagy, at least in the early phase, serves to protect cells from apoptosis. Additionally, we used chloroquine, a clinically approved antimalarial drug known to inactivate lysosomal functions, to interfere with the autophagic process. Chloroquine also accelerated apoptotic death induced by ADI. Our results suggest a protective role of autophagy in the initial phase of ADI-induced apoptosis, and the potential of using ADI/chloroquine combination therapy to enhance the killing of tumor cells.

The chemotherapeutic agent docetaxel represents one of the few options for treating hormone-resistant prostate cancer. Since docetaxel induces cell killing via caspases, leading to induction of traditional apoptosis, we determined *in vivo* whether ADI may complement docetaxel in cell killing via a caspase-independent mechanism. Whereas each therapy slowed growth of CWR22Rv1 xenografts, the ADI/docetaxel combination showed a dramatic reduction of tumor growth compared to the groups receiving individual therapies. Although we have yet to examine ADI/chloroquine combination therapy *in vivo*, chloroquine has emerged as an anti-cancer autophagy modulator in other *in vivo* models. Combination therapy is currently very attractive for several reasons. In addition to increased efficacy, combination therapy may circumvent or delay the emergence of resistant tumors or improve patient quality of life by reducing side effects associated with high concentrations of chemotherapy drugs.

In summary, we present a new therapy for prostate cancer, based on the interesting finding that most, if not all, prostate cancers are auxotrophic for arginine. At present, we do not understand why prostate cancer cells are selected against ASS expression, nor do we know the initial mechanism whereby ADI triggers autophagy and caspase-independent apoptosis. Increasing evidence suggests that autophagic death induced by metabolic stress utilizes pathways largely different from the caspase-dependent genotoxic agents. Targeting disparate mechanisms appears beneficial, implying that the interaction of autophagy and apoptosis has therapeutic rationale.

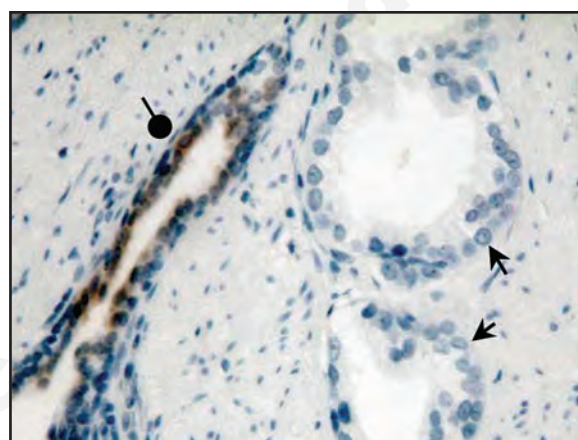


Figure 2. ASS expression in prostate cancer tissue by immunohistochemistry. ASS is readily expressed in benign prostate glands (round arrowhead) with heavy luminal staining by anti-ASS monoclonal antibody. In contrast, no ASS reactivity is detected in cancerous prostate glands (arrows).

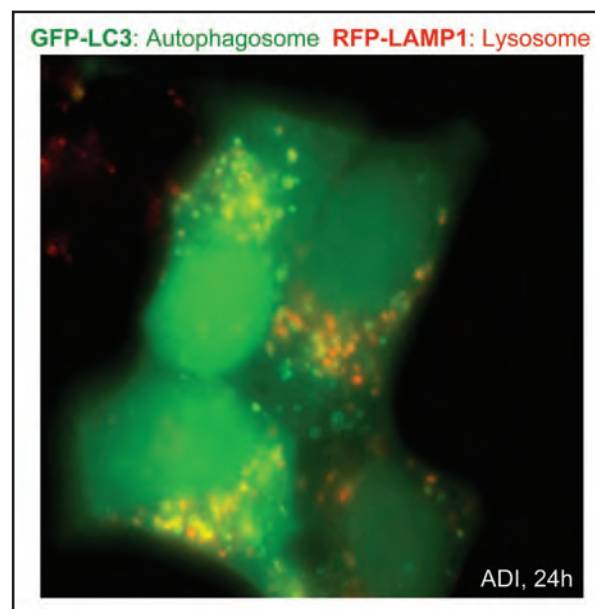


Figure 3. Autophagosome formation by ADI. CWR22Rv1 cells overexpressing GFP-LC3 and RFP-LAMP-1 labeled proteins were treated with 0.3 $\mu\text{g}/\text{mL}$ ADI for 24 hours. Individual autophagosomes (green), lysosomes (red), and the co-localization of both structures (yellow) are readily observed.